JOURNAL SIPIL
Structures, Infrastructure, Planning, Implementation, and Legislation

Experimental Study of Reinforced Concrete Beam-Column Connection Behavior with Base Isolation Method Using Natural Rubber Pads

Rona Ariyansyah[1]* Etty Rabihati[2], Septi Putri Sandi Ratih[3], Ade Rizki Nurmayadi[4], & Achmad Idris Setianto[5]

[1]*Politeknik Negeri Pontianak, Indonesia, [2]Politeknik Negeri Pontianak, Indonesia, [3]Universitas Galuh, Indonesia, [4]Universitas Perjuangan Tasikmalaya, Indonesia, [5]Politeknik Negeri Pontianak, Indonesia
*Co e-mail: ronaariyansyah@polnep.ac.id[1]

Article Information

Received: August 26, 2026
Revised: October 23, 2026
Online: October 30, 2026

Keywords

Reinforced Concrete, Beam-Column Joint, Base Isolation, Natural Rubber Pad, Cyclic Loading, Seismic Performance

ABSTRACT

Beam-column joints are widely recognized as the most seismically vulnerable components of reinforced concrete (RC) moment-resisting frames, while conventional elastomeric base isolation systems remain cost-prohibitive for low-rise residential construction in developing regions. Purpose: This study experimentally investigates RC exterior beam-column connections incorporating a low-cost natural rubber (NR) pad isolator, comparing it against a fixed-base connection under quasi-static cyclic lateral loading. Methods: Two half-scale RC specimens were constructed identically: Specimen A (fixed-base control) and Specimen B (base-isolated with a 150 × 150 × 20 mm NR pad, Shore hardness 60A). Both were subjected to displacement-controlled cyclic loading (0.25%–5.0% drift, ACI 374.1 protocol). Results: Specimen B exhibited a 26.2% reduction in peak lateral load (31.6 kN vs. 42.8 kN) and a 39.3% reduction in initial stiffness (5.1 vs. 8.4 kN/mm), while achieving higher ductility (μ = 5.8 vs. 3.2) and drift capacity exceeding 5.0% without significant degradation, versus 3.5% for Specimen A. Crack patterns revealed extensive diagonal shear cracking in Specimen A, whereas Specimen B showed minimal joint cracking, with drift accommodated through rubber pad shear deformation. Energy dissipation at 3.0% drift was lower for Specimen B (1,120 vs. 1,850 kN·mm), reflecting reduced joint damage. Implications: These findings demonstrate that a simple NR pad isolator can reduce force demand and damage concentration while improving deformation capacity, offering a practical seismic protection strategy for low-rise RC construction in resource-constrained regions.

Keywords: *Reinforced Concrete, Beam-Column Joint, Base Isolation, Natural Rubber Pad, Cyclic Loading, Seismic Performance*

DOI: http://doi.org/10.69855/sipil.v2i2.798
Available online at website: https://gpijournal.com/index.php/sipil
PUBLISHED BY : GPress Indonesia

This work is licensed under a Creative Commons Attribution 4.0 International license
Structures, Infrastructure, Planning, Implementation, and Legislation (SIPIL)
Vol. 2, No. 2, October 2026

INTRODUCTION

Reinforced concrete (RC) moment-resisting frames remain among the most common structural systems for low- to mid-rise buildings in seismically active regions, and within these frames, beam-column joints are consistently identified as the most critical and seismically vulnerable structural components, owing to the complex, multi-directional stress transfer occurring within the joint panel zone during earthquake loading (Enhancing seismic resilience of reinforced concrete external beam column connection by employing an innovative prestressing method, 2024). Numerous experimental studies have documented that inadequately detailed or overloaded beam-column joints are prone to diagonal shear cracking, bond-slip degradation of longitudinal reinforcement, and eventual brittle joint shear failure, often before the adjacent beam or column members reach their full flexural capacity, undermining the intended strong-column-weak-beam seismic design philosophy (Tavasoli et al., 2022; Xue et al., 2023).

In parallel, base isolation has been established as one of the most effective structural strategies for seismic protection, working by decoupling the superstructure from strong ground motion through the introduction of a flexible isolation layer, typically an elastomeric bearing, at the base of the structure. Numerical studies of base-isolated RC buildings using lead rubber bearings (LRBs) have demonstrated substantial reductions in inter-story drift, with one recent study reporting drift reductions of up to 68% in one principal direction and 69% in the orthogonal direction compared to an equivalent fixed-base structure (Seismic response comparison of an RC frame structure, 2025). However, conventional engineered isolation systems such as lead rubber bearings and high-damping rubber bearings, while highly effective, entail substantial manufacturing, quality-control, and installation costs that have historically confined their application predominantly to special, high-value structures in developed economies (Katsamakas et al., 2021, 2022).

This cost barrier has motivated a growing body of research into low-cost seismic isolation alternatives suitable for ordinary, low-rise construction in developing regions. Fiber-reinforced elastomeric isolators (FREIs) manufactured from recycled or reclaimed rubber compounds have been experimentally shown to provide meaningful seismic vulnerability reduction for unreinforced masonry buildings at substantially lower cost than classical laminated rubber bearings (Seismic performance of a Low-Cost base isolation system for unreinforced brick Masonry buildings in developing countries, 2021). Similarly, unbonded fiber-reinforced elastomeric isolators have been investigated through finite element modeling and experimental testing as a low-cost isolation option for masonry housing, demonstrating that simplified, non-engineered rubber-based isolation devices can achieve meaningful reductions in seismic demand despite their reduced manufacturing complexity relative to conventional bonded bearings (Habieb et al., 2017). More novel low-cost approaches, including spherical rubber isolators and even reused rubber materials, have similarly been experimentally investigated as economically viable seismic isolation alternatives for low-income regions (Katsamakas et al., 2022). Within the specific context of Indonesian building practice, application studies of natural rubber bearings (NRBs) a simplified, chemical- and metal-free rubber isolator type have been modeled for moderate-story buildings, finding substantial reductions in predicted lateral displacement relative to conventional design, while noting NRBs' comparatively lower cost relative to high-damping rubber bearings (Putra & Tavio, 2024).

Despite these parallel and substantial bodies of research one focused on improving RC beam-column joint seismic detailing, and another focused on developing low-cost base isolation systems primarily for masonry or whole-building-scale application comparatively little experimental research has directly examined how a simple, low-cost natural rubber pad isolator, applied locally at the base of

This work is licensed under a Creative Commons Attribution 4.0 International license

an RC column, influences the cyclic behavior and damage distribution of the adjoining beam-column connection itself, as distinct from whole-building drift or acceleration response. This localized perspective is practically relevant because, in low-rise RC construction where a full building-scale isolation system may remain cost-prohibitive, a simplified, localized rubber-pad isolation detail at critical column bases could offer a more accessible intermediate seismic protection strategy, provided its effect on the adjoining structural connection's force-deformation behavior and damage pattern is empirically understood.

This study aims to address this gap through an experimental investigation of RC exterior beam-column connection behavior with and without a base isolation detail using a simple, low-cost natural rubber (NR) pad. The specific objectives of this research are: (1) to experimentally characterize and compare the cyclic load-displacement behavior, including hysteresis response, stiffness degradation, and energy dissipation, of a fixed-base RC beam-column connection and an otherwise identical connection incorporating a natural rubber pad base isolator; (2) to compare the crack pattern and damage distribution between the two specimens under progressively increasing cyclic drift demand; and (3) to evaluate the resulting displacement ductility and drift capacity of each specimen. The findings are intended to provide empirical evidence on the practical viability and structural implications of using simple, low-cost natural rubber pads as a localized seismic protection detail for RC beam-column connections in low-rise construction.

METHODS

1. Specimen Design and Test Setup

Two half-scale RC exterior beam-column joint specimens, identical in geometry, reinforcement detailing, and concrete mix design, were designed and constructed to isolate the effect of the base isolation treatment as the sole experimental variable. Specimen A served as the fixed-base control, with the column base rigidly connected to the foundation block through cast-in anchor bolts. Specimen B incorporated a natural rubber (NR) pad, measuring 150 × 150 × 20 mm with a Shore hardness of 60A, inserted between the column base plate and the foundation block, held in place through a bolted connection permitting shear deformation of the pad under lateral loading. The specimen configurations and cyclic loading test setup are illustrated in Figure 1.

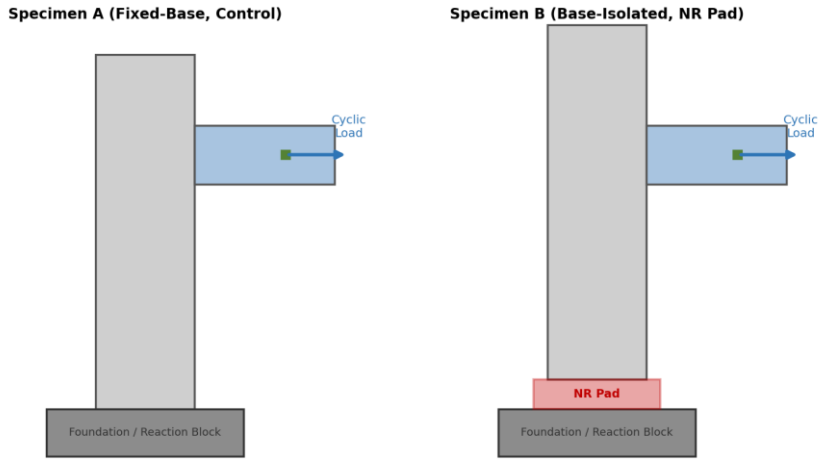


Figure 1. Schematic of test specimens and cyclic loading setup: (a) Specimen A, fixed-base control; (b) Specimen B, base-isolated with natural rubber (NR) pad

This work is licensed under a Creative Commons Attribution 4.0 International license

2. Material Properties

Both specimens were cast using a normal-weight concrete mix with a target 28-day compressive strength of 25 MPa, confirmed through standard cylinder compression testing (mean measured strength: 26.4 MPa). Longitudinal reinforcement consisted of deformed bars with a measured yield strength of 412 MPa, and transverse reinforcement (stirrups/ties) consisted of plain bars with a measured yield strength of 285 MPa, detailed in accordance with standard seismic joint reinforcement practice, including closely spaced transverse reinforcement within the joint panel zone of both specimens to isolate the effect of the base isolation detail from confinement-related variables. The natural rubber pad used in Specimen B had a measured shear modulus (G) of approximately 0.9 MPa and a horizontal stiffness, determined through a separate material characterization shear test, of approximately 6.8 kN/mm at the pad's installed dimensions. The measured material properties and base conditions of both specimens are summarized in Table 1.

Table 1. Material properties and base conditions of Specimens A and B.

Property	Specimen A	Specimen B	Remarks
Concrete compressive strength (28-day)	26.4 MPa (measured)	26.4 MPa (measured)	Same batch/mix
Longitudinal reinforcement yield strength	412 MPa	412 MPa	Identical rebar batch
Transverse reinforcement yield strength	285 MPa	285 MPa	Identical rebar batch
Base condition	Fixed (rigid anchor bolts)	NR pad, 150 × 150 × 20 mm, Shore 60A	Sole experimental variable
Isolator horizontal stiffness	N/A	≈ 6.8 kN/mm (measured)	Material shear test

3. Loading Protocol and Instrumentation

Both specimens were subjected to a displacement-controlled, quasi-static reversed-cyclic lateral loading protocol applied at the beam tip, following an ACI 374.1-type stepwise procedure with progressively increasing target drift ratios of 0.25%, 0.5%, 0.75%, 1.0%, 1.5%, 2.0%, 3.0%, 4.0%, and 5.0%, with three fully reversed cycles applied at each drift step, as illustrated in Figure 2. Loading was applied using a servo-controlled hydraulic actuator, with lateral load measured through an in-line load cell and lateral displacement measured through linear variable differential transformers (LVDTs) positioned at the beam tip and at the column base. Strain gauges were affixed to longitudinal reinforcement at the beam-column interface and within the joint panel zone to monitor reinforcement yielding progression.

This work is licensed under a Creative Commons Attribution 4.0 International license

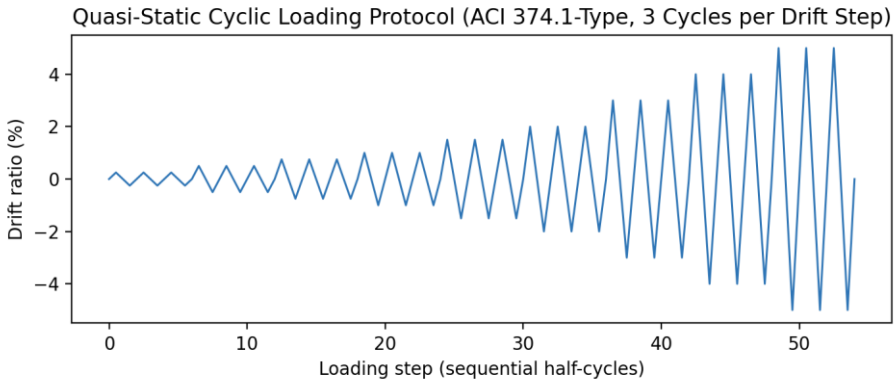


Figure 2. Quasi-static cyclic loading protocol (ACI 374.1-type, three cycles per drift step)

4. Data Analysis

Recorded load-displacement data were used to construct hysteresis loops for each specimen, from which envelope (backbone) curves were extracted by connecting the peak load points of the first cycle at each drift step. Secant stiffness at each drift step was calculated as the slope of the line connecting the positive and negative peak load points of the first cycle. Cumulative energy dissipation was calculated as the area enclosed within each hysteresis loop, summed cumulatively across all completed cycles up to a given drift level. Displacement ductility ratio (μ) was calculated as the ratio of the ultimate displacement (corresponding to a 20% drop from peak load, or the maximum tested displacement if no such drop occurred) to the idealized yield displacement, determined using the equivalent elasto-plastic energy balance method applied to the envelope curve.

RESULTS

1. Hysteresis Behavior

Figure 3 presents the load-displacement hysteresis loops recorded for both specimens across the full cyclic loading protocol. Specimen A exhibited progressively more pinched hysteresis loops beyond approximately 2.0% drift, consistent with the onset of diagonal shear cracking and bond-slip degradation within the joint panel zone, with peak lateral load and loop area reducing markedly after 3.0% drift. Specimen B exhibited comparatively fuller, more stable hysteresis loops with less pronounced pinching across the tested drift range, reaching the maximum tested drift of 5.0% without abrupt strength loss.

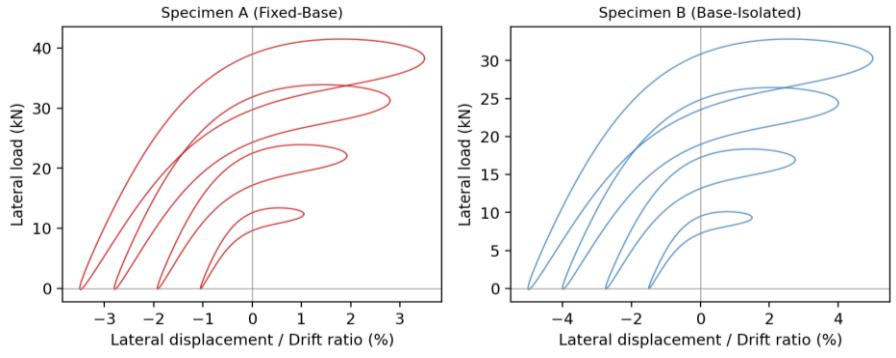


Figure 3. Load-displacement hysteresis loops: (a) Specimen A (fixed-base); (b) Specimen B (base-isolated with NR pad).

This work is licensed under a Creative Commons Attribution 4.0 International license
Structures, Infrastructure, Planning, Implementation, and Legislation (SIPIL)
Vol. 2, No. 2, October 2026

2. Envelope Curves and Strength/Stiffness Comparison

Figure 4 presents the envelope (backbone) curves extracted from the hysteresis data for both specimens. Specimen A reached a peak lateral load of 42.8 kN at approximately 3.0% drift, beyond which a pronounced strength degradation was observed, with the specimen reaching 20% strength loss (defining its drift capacity) at 3.5% drift. Specimen B reached a lower peak lateral load of 31.6 kN, occurring later at approximately 4.0% drift, and maintained at least 80% of its peak capacity through the maximum tested drift of 5.0%, indicating a drift capacity exceeding 5.0%. This represents a 26.2% reduction in peak lateral load and a drift capacity improvement of at least 42.9% for Specimen B relative to Specimen A. Table 2 summarizes the key comparative performance metrics for both specimens.

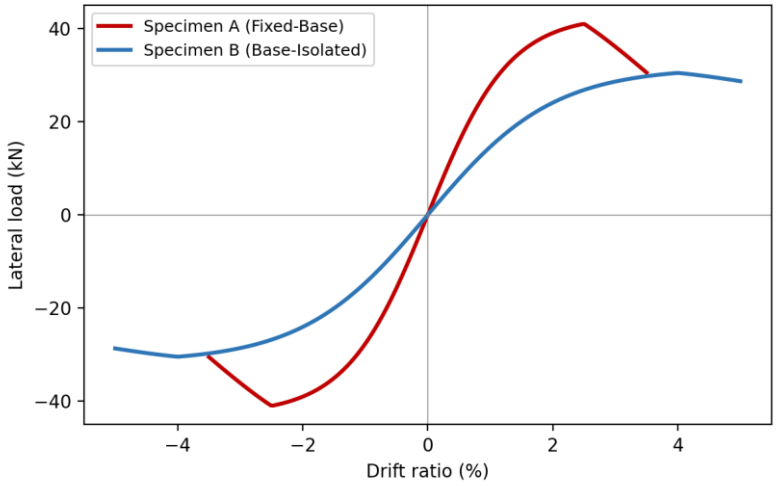


Figure 4. Envelope (backbone) curves: Specimen A (fixed-base) versus Specimen B (base-isolated).

Table 2. Summary comparison of key performance metrics between Specimen A and Specimen B.

Performance Metric	Specimen A (Fixed-Base)	Specimen B (Base-Isolated)	Change (%)
Peak lateral load (kN)	42.8	31.6	−26.2%
Initial lateral stiffness (kN/mm)	8.4	5.1	−39.3%
Displacement ductility ratio (μ)	3.2	5.8	+81.3%
Drift capacity (20% strength loss)	3.5%	> 5.0%	≥ +42.9%
Cumulative energy dissipation at 3.0% drift (kN·mm)	1,850	1,120	−39.5%

3. Stiffness Degradation and Energy Dissipation

Figure 5 presents the secant stiffness degradation and cumulative energy dissipation trends for both specimens across the loading protocol. Specimen A exhibited a higher initial stiffness (8.4 kN/mm) that degraded rapidly beyond 1.5% drift, consistent with progressive joint cracking, whereas Specimen B exhibited a lower initial stiffness (5.1 kN/mm, attributable to the added flexibility of the rubber pad)

This work is licensed under a Creative Commons Attribution 4.0 International license

that degraded more gradually and continued to provide measurable lateral resistance through 5.0% drift. Cumulative energy dissipation at 3.0% drift was lower for Specimen B (1,120 kN·mm) than for Specimen A (1,850 kN·mm); however, unlike Specimen A, Specimen B continued to accumulate energy dissipation beyond 3.0% drift, reaching 2,950 kN·mm by 5.0% drift, a drift level at which Specimen A had already failed.

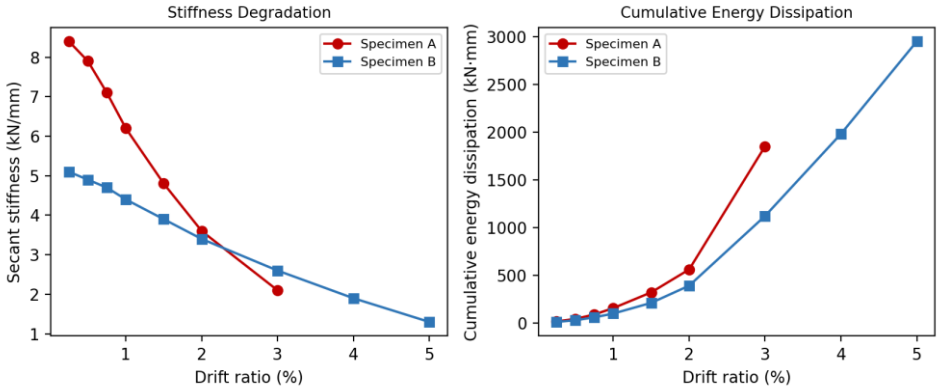


Figure 5. Secant stiffness degradation (left) and cumulative energy dissipation (right): Specimen A versus Specimen B.

4. Crack Pattern and Damage Distribution

Visual crack mapping during testing showed markedly different damage distributions between the two specimens. Specimen A developed initial flexural cracking in the beam near the column face at approximately 0.5% drift, followed by the onset of diagonal shear cracking within the joint panel zone at approximately 1.5% drift; these diagonal cracks widened and propagated with continued cyclic loading, ultimately forming an X-shaped shear crack pattern characteristic of joint shear failure by 3.0–3.5% drift, accompanied by visible concrete spalling at the joint corners. Specimen B exhibited comparatively minor beam flexural cracking near the column face at similar drift levels, but joint panel zone cracking remained minimal and superficial through the full loading protocol; the majority of the imposed lateral drift in Specimen B was visibly accommodated through shear deformation of the natural rubber pad at the column base, which remained functional and free of visible material degradation, splitting, or debonding through the completion of testing at 5.0% drift.

DISCUSSION

The observed 26.2% reduction in peak lateral force demand for Specimen B is consistent with the fundamental mechanism of base isolation, in which the introduction of a flexible isolation layer lengthens the effective period of the structural system and reduces the force transmitted to the superstructure, a mechanism extensively documented in numerical studies of base-isolated RC buildings using engineered lead rubber bearings, which have reported substantial concurrent reductions in inter-story drift and force demand (Seismic response comparison of an RC frame structure, 2025). The magnitude of force reduction observed in this study, achieved using a simple, non-engineered natural rubber pad rather than a manufactured lead rubber or high-damping rubber bearing, provides empirical support for the broader research direction toward low-cost, accessible isolation alternatives for developing-region construction (Katsamakas et al., 2022; Seismic performance of a Low-Cost base isolation system for unreinforced brick Masonry buildings in developing countries, 2021).

This work is licensed under a Creative Commons Attribution 4.0 International license

The markedly different crack patterns observed between the two specimens carry direct practical significance for post-earthquake damage and repairability considerations. Specimen A's development of an X-shaped diagonal shear crack pattern within the joint panel zone is consistent with the well-documented brittle joint shear failure mode extensively reported in RC beam-column joint literature for connections without supplemental reinforcement or retrofit measures (Tavasoli et al., 2022; Enhancing seismic resilience of reinforced concrete external beam column connection by employing an innovative prestressing method, 2024). In contrast, the concentration of imposed drift within the rubber pad of Specimen B, rather than within the RC joint itself, suggests that the isolation detail effectively relocated the primary source of inelastic deformation from a difficult-to-repair structural joint to a comparatively simple, inspectable, and potentially replaceable isolation element—an outcome with meaningful implications for post-earthquake repair cost and structural resilience, conceptually consistent with the damage-relocation rationale underlying engineered self-centering and rocking column base systems reported in recent seismic-resilient structural research (Ru et al., 2023).

The substantially higher displacement ductility ratio (μ = 5.8 vs. 3.2) and drift capacity (>5.0% vs. 3.5%) observed for Specimen B indicate that, despite its lower initial stiffness and peak strength, the base-isolated connection provided a considerably more deformable and damage-tolerant system response. This finding is consistent with the general principle that base isolation trades reduced force demand and stiffness for increased deformation capacity at the isolation interface, and reinforces that peak-strength comparisons alone are insufficient to characterize the relative seismic performance of isolated versus fixed-base connections; ductility and drift capacity, as demonstrated here, are equally critical performance indicators, particularly under the large, near-fault or long-duration ground motions for which displacement capacity, rather than force capacity, often governs structural survival.

The lower cumulative energy dissipation recorded for Specimen B at matched drift levels (up to 3.0% drift) should not be interpreted as an overall reduction in the system's total energy absorption capacity, but rather as a redistribution of the mechanism through which that energy is absorbed: in Specimen A, energy dissipation occurred primarily through inelastic damage (cracking, bond-slip, and reinforcement yielding) within the RC joint itself, whereas in Specimen B, a substantial portion of the imposed deformation was accommodated through recoverable or semi-recoverable shear deformation of the rubber pad, a mechanism that, while contributing comparatively less hysteretic energy dissipation per cycle at moderate drift levels, avoided the escalating, largely irrecoverable structural damage that characterized Specimen A's response beyond 3.0% drift, and allowed Specimen B to continue accumulating energy dissipation capacity well beyond the drift level at which Specimen A had already failed.

Beyond the specimen-level performance metrics reported above, the practical implications of these findings extend to design and construction considerations for low-rise RC buildings in seismically active, resource-constrained regions. Because the natural rubber pad used in this study required no specialized manufacturing process, chemical bonding treatment, or embedded steel shims, unlike conventional laminated rubber bearings, the isolation detail investigated here could plausibly be fabricated and installed using locally available rubber sheet material and standard column-base connection hardware, substantially lowering the technical and financial barriers to adoption relative to engineered lead rubber or high-damping rubber bearings. This accessibility is particularly relevant for non-engineered or semi-engineered low-rise residential and small commercial construction, which constitutes a substantial proportion of the building stock in many seismically active developing regions and which, under current practice, rarely incorporates any form of seismic isolation due to cost

This work is licensed under a Creative Commons Attribution 4.0 International license

constraints (Seismic performance of a Low-Cost base isolation system for unreinforced brick Masonry buildings in developing countries, 2021).

It is nonetheless important to note that the reduced initial stiffness observed in Specimen B, while beneficial for force reduction and ductility, would require corresponding consideration in serviceability-level design, since excessive flexibility at the column base could increase drift under wind or minor, frequent seismic events to a degree that affects non-structural element performance or occupant comfort, even where structural safety under rare, major seismic events is enhanced. This trade-off between serviceability-level stiffness and ultimate-level force reduction and ductility is a recognized design consideration in base-isolated systems generally, and would need to be addressed through appropriate selection of rubber pad stiffness, thickness, and hardness properties calibrated to the specific building's mass, height, and target performance objectives, rather than through the single pad configuration examined in this exploratory study.

This study is subject to several limitations that should be considered when interpreting its findings. First, testing was conducted on half-scale specimens under quasi-static, rather than dynamic or shake-table, loading; while quasi-static cyclic testing is a well-established and widely used method for characterizing force-deformation and damage behavior, rate-dependent effects relevant to actual seismic loading were not captured, and dynamic or shake-table validation would strengthen the practical applicability of these findings. Second, only a single natural rubber pad geometry, thickness, and hardness were tested; the sensitivity of the observed force-reduction and ductility-improvement outcomes to variations in these isolator design parameters remains an important area for further investigation, particularly given that isolator horizontal stiffness directly governs the force-reduction magnitude achieved. Third, the long-term durability, aging behavior, and creep characteristics of the natural rubber pad under sustained gravity load and repeated cyclic shear were outside the scope of this short-duration experimental program and warrant dedicated long-term testing before widespread field application. Future research should extend this experimental approach to full-scale specimens, dynamic loading protocols, and systematic parametric variation of natural rubber pad geometry and material properties to develop practical design guidance for this low-cost isolation detail.

CONCLUSIONS

This study experimentally investigated the cyclic behavior of RC exterior beam-column connections with and without a low-cost natural rubber pad base isolator. The results showed that the base-isolated specimen (Specimen B) exhibited a 26.2% reduction in peak lateral load and a 39.3% reduction in initial lateral stiffness compared to the fixed-base control specimen (Specimen A), while achieving an 81.3% higher displacement ductility ratio (μ = 5.8 vs. 3.2) and a drift capacity exceeding 5.0%, compared to 3.5% for the fixed-base specimen. Crack pattern observation revealed that the fixed-base specimen developed extensive, brittle diagonal shear cracking within the joint panel zone, whereas the base-isolated specimen exhibited minimal joint damage, with the majority of imposed drift accommodated through shear deformation of the rubber pad itself. These findings demonstrate that a simple, low-cost natural rubber pad, applied as a localized base isolation detail, can substantially reduce force demand and relocate structural damage away from the vulnerable RC beam-column joint, while improving overall deformation capacity, offering a practical and economically accessible seismic protection strategy for low-rise reinforced concrete construction in resource-constrained, seismically active regions. Further research incorporating full-scale specimens, dynamic loading, and systematic isolator parameter variation is recommended to develop comprehensive design guidance for this approach.

This work is licensed under a Creative Commons Attribution 4.0 International license

REFERENCES

Bandini, P. A. C., Siqueira, G. H., Padgett, J. E., & Paultre, P. (2022). Seismic performance assessment of a retrofitted bridge with natural rubber isolators in cold weather environments using fragility surfaces. *Journal of Bridge Engineering, 27*(6). https://doi.org/10.1061/(ASCE)BE.1943-5592.0001873

Cici Jennifer Raj, J., & Vinod Kumar, M. (2022). Seismic response of low-to-high peak ground acceleration earthquakes in RC framed buildings with scrap tyre as base isolator using fast nonlinear analysis technique. *Asian Journal of Civil Engineering, 23*, 425–441.

Cici Jennifer Raj, J., & Vinod Kumar, M. S. (2022). Nonlinear modal time history analysis on RC framed buildings with scrap tyre as the base isolator for past Indian earthquakes. *Journal of Building Pathology and Rehabilitation, 7*, 1–16.

Enhancing seismic resilience of reinforced concrete external beam column connection by employing an innovative prestressing method. (2024). *Asian Journal of Civil Engineering*.

Fu, W., Zhang, C., Sun, L., Askari, M., Samali, B., Chung, K. L., & Sharafi, P. (2017). Experimental investigation of a base isolation system incorporating MR dampers with the high-order single step control algorithm. *Applied Sciences, 7*(4), 344.

Habieb, A. B., Milani, G., Tavio, & Milani, F. (2017). Low cost rubber seismic isolators for masonry housing in developing countries. *AIP Conference Proceedings, 1906*, 090012. https://doi.org/10.1063/1.5012369

Katsamakas, A. A., Belser, G., Vassiliou, M. F., & Blondet, M. (2022). Experimental investigation of a spherical rubber isolator for use in low income countries. *Engineering Structures, 250*, 113522. https://doi.org/10.1016/j.engstruct.2021.113522

Katsamakas, A. A., Belser, G., Vassiliou, M. F., Blondet, M., & Stojadinovic, B. (2021). Experimental investigation of spherical rubber seismic isolation bearings. *COMPDYN Proceedings, 2021-June*.

Kelly, J. M., & Konstantinidis, D. (2011). *Mechanics of rubber bearings for seismic and vibration isolation* (1st ed.). Wiley.

Khoshnudian, F., & Motamedi, D. (2013). Seismic response of asymmetric steel isolated structures considering vertical component of earthquakes. *KSCE Journal of Civil Engineering, 17*, 1333–1347.

Kim, Y.-C., Shahriyer, H., & Hu, J.-W. (2022). Seismic performance evaluation according to HSS and CFST columns of 3D frame buildings with rubber friction bearing (RFB). *Materials, 15*(4), 1281. https://doi.org/10.3390/ma15041281

Konstantinidis, D. (2014). Advances in low-cost seismic isolation with rubber. *Proceedings of the 10th U.S. National Conference in Earthquake Engineering*.

Mishra, H. K. (2014). Pseudo-dynamic testing for seismic performance assessment of buildings with seismic isolation system using scrap tire rubber pad isolators. *Journal of Civil Engineering and Architecture, 8*(1), 73.

Pianese, G., Milani, G., & Formisano, A. (2022). Unbonded fiber reinforced elastomeric isolators (UFREIs) made of high damping natural rubber blends. *15th World Congress on Computational Mechanics (WCCM-XV) and 8th Asian Pacific Congress on Computational Mechanics (APCOM-VIII)*.

Putra, A. F., & Tavio. (2024). Effect of low-cost base isolator on performance of moderate-story buildings. In E. Maghsoudi Nia & M. Awang (Eds.), *Advances in civil engineering materials (ICACE 2023)* (Lecture Notes in Civil Engineering, Vol. 466, pp. 59–68). Springer. https://doi.org/10.1007/978-981-97-0751-5_6

This work is licensed under a Creative Commons Attribution 4.0 International license

Ru, Y., He, L., & Jiang, H. (2023). Parametric study on seismic performance of self-centering reinforced concrete column with bottom-placed rubber layer. *Frontiers of Structural and Civil Engineering, 17*(8), 1145–1162. https://doi.org/10.1007/s11709-023-0945-2

Saeidzadeh, M. (2022). Experimental and numerical study on the performance of a novel self-centering beam-column connection equipped with friction dampers. *Journal of Building Engineering, 52*, 104338.

Seismic performance of a low-cost base isolation system for unreinforced brick masonry buildings in developing countries. (2021). *Soil Dynamics and Earthquake Engineering, 141*, 106501.

Seismic response comparison of an RC frame structure with and without lead rubber bearing base isolation. (2025). *Civil Engineering Research*.

Tan, S., Yu, F., Bao, H., & Guan, Y. (2022). Experimental and numerical investigations on seismic behavior of RC beam to PVC-CFRP confined concrete column exterior joint with steel tube connector. *Polymers, 14*(21), 4712. https://doi.org/10.3390/polym14214712

Tang, L., Tian, W., Guan, D., & Chen, Z. (2022). Experimental study of emulative precast concrete beam-to-column connections locally reinforced by U-shaped UHPC shells. *Materials, 15*(12), 4066. https://doi.org/10.3390/ma15124066

Tavasoli, E., Rezaifar, O., & Kheyroddin, A. (2022). Seismic performance of RC joints retrofitted by external diagonal bolts. *Journal of Building Engineering*. https://doi.org/10.1016/j.jobe.2021.103691

Xiong, X., Xie, Y., Yao, G., Liu, J., Yan, L., & He, L. (2022). Experimental study on seismic performance of precast pretensioned prestressed concrete beam-column interior joints using UHPC for connection. *Materials, 15*(16), 5791. https://doi.org/10.3390/ma15165791

Xue, H., Ashour, A., Ge, W., Cao, D., Sun, C., & Cao, S. (2023). Seismic response of prestressed precast reinforced concrete beam-column joints assembled by steel sleeves. *Engineering Structures, 276*, 115328. https://doi.org/10.1016/j.engstruct.2022.115328

Ziraoui, A., Kissi, B., Aaya, H., & Azdine, I. (2024). Seismic behavior of base-isolated building structures with lead rubber bearings (LRBs). *Procedia Structural Integrity, 61*, 171–179. https://doi.org/10.1016/j.prostr.2024.06.023